An Experimental Study on Velocity Profiles and Turbulence Intensity of Developing Turbulent Pulsating Flows in the Entrance Region of a Square Duct

G.M. Park*, Y.H. Koh*

Abstract

The flow characteristics of developing turbulent pulsating flows are investigated experimentally in the entrance region of a square duct (40 mm×40 mm and 4,000 mm). Mean velocity profiles, turbulence intensity and entrance length are measured by using a hot-wire anemometer system together with data acquisition and processing systems. It is found that the velocity waveforms are not changed in the fully developed flow region where that $x/D_h \geq 40$. For turbulent pulsating flow, the turbulent components in the velocity waveforms increase as the dimensionless transverse position approaches the wall. Mean velocity profiles of the turbulent steady flows follow the one-seventh power law profile in the fully developed flow region. Turbulence intensity increases as the dimensionless transverse position increases from the center to the wall of the duct, and is slightly smaller in the accelerating phase than in the decelerating phase for the turbulent pulsating flows. The entrance length of the turbulent pulsating flow is about 40 times as large as the hydraulic diameter under the present experimental conditions.

Nomenclature

A_1 : Velocity amplitude ratio($=|\bar{u}_{m,os,1}|/\bar{u}_{m,ta}$)
A_p : Piston stroke of oscillator(mm)
a : Duct half-width(mm)
b : Duct half-width(mm)
D_h : Hydraulic diameter($=4ab/2(a+b)$)(mm)
f : Frequency of oscillation(Hz)
L_e : Entrance length(mm)
Re : Reynolds number
t : Time(s)
u, v, w : Velocity component along x-, y-, and z-axis respectively(m/s)
x, y, z : Cartesian coordinates of test section
x' : Dimensionless x-axis($=\nu x/ab\bar{u}_m$)
y' : Dimensionless y-axis($=y/a$)
z' : Dimensionless z-axis($=z/b$)

Subscripts And Others

ν : Molecular kinematic viscosity(m^2/s)
ρ : Density(Kg/m^3)
τ : Shear stress(Kg_f/m^2)
ω : Angular frequency of oscillation(rad/s)
ω^+ : Dimensionless angular frequency $[(D_h/2)\sqrt{\omega/\nu}]$
ω' : Dimensionless angular frequency $[(D_h/2)^2 \cdot \omega/\nu]$
os : Oscillatory component
rms : Root mean square value
ta : Instantaneous time-averaged value of a period
: Mean value

*Chosun Univ.

1. Introduction

In the entrance region of a duct connected with reciprocating fluid machinery turbulent pulsating flow is frequently encountered. And turbulent pulsating flows are divided into developing and fully developed processes. Thus flow analysis in the entrance region must be studied in detail. Because this analysis of the pulsating flow is not only used as basic data in the design of fluid mechinery but is also applied very usefully in analyzing flows in the operation of fluid machinery such as pulsating combustion and pulsed jet engines, compressors, gas turbines, heat exchangers and duct systems of air conditioning system.

Gessner et al [2] analyzed experimentally obtained data of turbulent developing mean flow in the entrance region of a square duct. McComas[2] studied hydrodynamic entrance length using a general method in the duct flow with an arbitrary section.

From previous research,[3~8] it is seen that much study on steady flow has been achieved, but studies on pulsating flow have been only a few, concerning laminar and transitional flows and the study on turbulent pulsating flow has been limited to the circular pipe and fully developed flow region. Especially Ohmi's research team[3~6] experimentally investigated frictional loss and velocity profiles only in a circular pipe. For this reason we have recognized the necessity of accurate analysis for pulsating flow in entrance regions and have made an experimental analysis of the flow characteristics of developing turbulent pulsating flows in the entrance region of a square duct. Thus, the flow characteristics such as mean velocity profile, turbulence intensity distribution and entrance length that are obtained experimentally while constantly changing the location of crossing direction (z') and axial direction (x/D_h) along with the changes of velocity amplitude ratio (A_1), dimensionless angular frequency (ω^+) and Reynolds number of pulsating flow (Re_{ta}).

2. Experiments

2.1 Experimental Apparatus

A schematic diagram of the experimental apparatus is shown in Fig. 1. The experimental apparatus consists of a tested square duct, a scotch-yoke type oscillator, a three-dimensional traversing mechanism which can automatically traverse with variations along the x-, y- and z-axes, an orifice to measure flowrate, a blower and a variable-speed motor which can arbitrarily control the frequency of oscillatory flow. The scotch-yoke type osicillator driven by means of a suitable combination of a variable speed motor generates an oscillating flow.

An acryl resin square duct of the aspect ratio 1 was used in this experiment, its cross-section ($2a \times 2b$) was 40×40 mm and its length (L) 4000 mm. The upper duct (28-ϕ5.4 Drill, Tap 1/4") and both sides of the duct (64-ϕ1.0 Drill) were penetrated with a drill in order to measure velocity by means of the hot-wire anemometer.

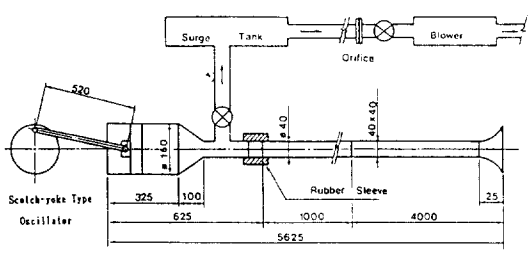

Fig. 1 Schematic diagram of experimental apparatus

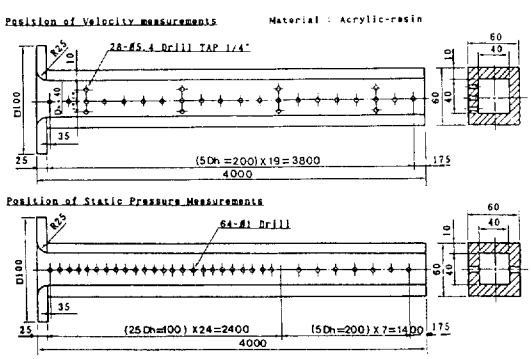

Fig. 2 Position of velocity and static pressure measurements

2.2 Experimental Procedures

A pulsatile flow is an oscillatory flow which is produced by a scotch-yoke type oscillator superimposed on a steady flow which is produced by a blower. Therefore the velocity control of steady flow progresses by means of a flowrate control valve which is set up between a surge tank and the blower. The turbulent pulsating flow has the following momentum balance equation as a basic equation for investigating the flow pattern.[9]

$$\rho\frac{d\bar{u}_m}{dt}+\frac{4}{D_h}\bar{\tau}_w=\frac{\Delta\bar{P}}{1} \tag{1}$$

$$\bar{u}_m=\bar{u}_{m,ta}+\sum_{n=1}^{\infty}\bar{u}_{m,os,n}\cdot\cos\{n\omega t+\angle(\bar{u}_{m,os,n})\} \tag{2}$$

Because the finite Fourier expansions with the fundamental expansions with the fundamental wave show good agreement with experimental data obtained here, we adopted the following equations with the fundamental wave for the turbulent pulsating flow. Of course, higher harmonics up to 6 are obtained for more general cases, but error was inside 5 percent.

$$\bar{u}_m=\bar{u}_{m,ta}+\bar{u}_{m,os,1}\cos\{\omega t+\angle(\bar{u}_{m,os,1})\} \tag{3}$$

Table 1 Experimental conditions for developing turbulent pulsating flow

x/D_h	f(Hz)	ω^+	A_p(mm)	$Re_{,os}$	$Re_{,ta}$	A_1
5	2.08	18.79	50	20000	16600	1.2
					33200	0.6
			115	46900	66400	0.7
10	2.08	18.79	50	20000	16600	1.2
					33200	0.6
			115	46900	66400	0.7
20	2.08	18.79	50	20000	16600	1.2
					33200	0.6
			115	46900	66400	0.7
30	2.08	18.79	50	20000	16600	1.2
					33200	0.6
			115	46900	66400	0.7
40	2.08	18.79	50	20000	16600	1.2
					33200	0.6
			115	46900	66400	0.7
50	2.08	18.79	50	20000	16600	1.2
					33200	0.6
			115	46900	66400	0.7
60	2.08	18.79	50	20000	16600	1.2
					33200	0.6
			115	46900	66400	0.7
90	2.08	18.79	50	20000	16600	1.2
					33200	0.6
			115	46900	66400	0.7

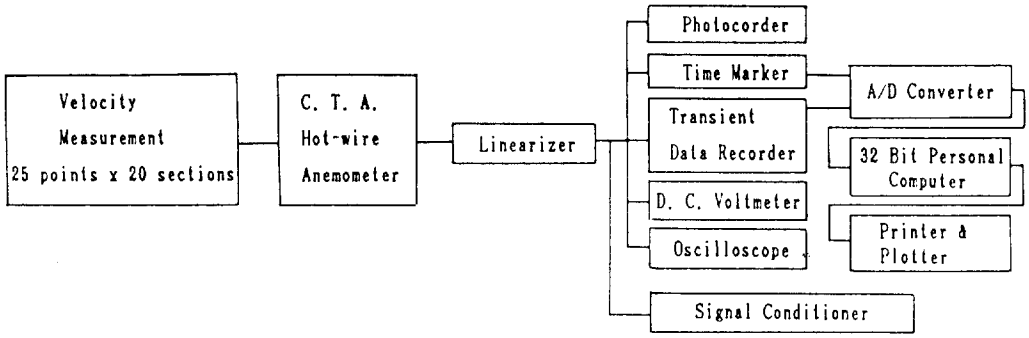

Fig. 3 Diagram of data acquisition and processing system

The pulsating flow is specified by the changes in velocity amplitude ratio (A_1), dimensionless angular frequency (ω^+) and time-averaged Reynolds number. Measurements of velocity and turbulent intensity for pulsating flow were made at $z'=0.0$, 0.3, 0.5, 0.7, 0.9 and 0.95 across the cross-section of the dimensionless axial positions ($x/D_h=5$, 10, 20, 30, 40, 50, 60). Measurements for the turbulent pulsating flow were also made until the position of axial direction where the velocity waveforms were not remained almost in invariant. Table 1 gives the list of these experimental conditions for developing turbulent pulsating flow.

These data were analyzed by a personal computer connected to an A/D converter using a signal conditioner, linearizer and anemometer correlator. The time-averaged Reynolds number for turbulent pulsating flow was calculated by means of this equation ($Re_{ta}=\overline{u}_{m,ta}\cdot D_h/\nu$)/ The dimensionless angular frequency and velocity amplitude ratio were obtained from $\omega^+=(D_h/2)\sqrt{\omega/\nu}$ and $A_1=|\overline{u}_{m,os,1}|/|\overline{u}_{m,ta}|$.

3. Results and Discussion

3.1 Mean velocity profile and turbulence intensity distributions

The mean velocity profile and turbulence inten-

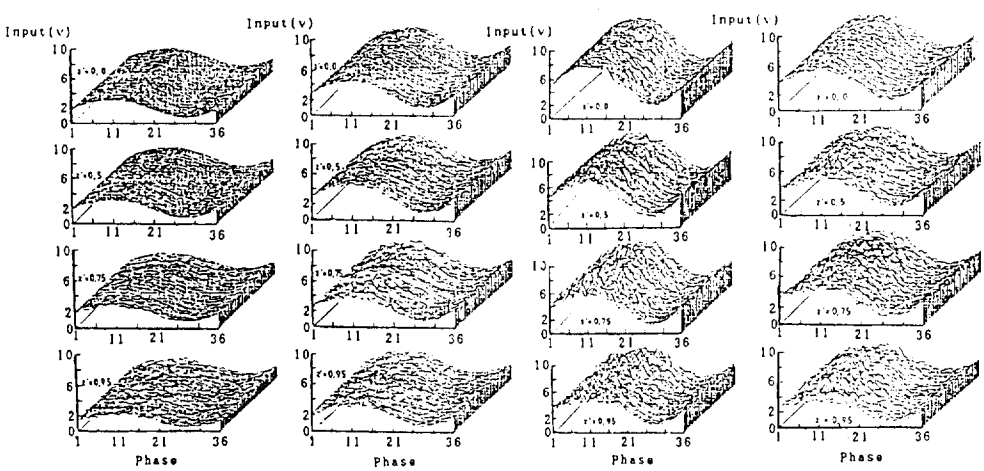

Fig. 4 Velocity waveforms of developing turbulent pulsating flows at $Re_{ta}=66400$ and $Re_{os}=46900$

sity distributions are shown in Figs. 4~13. Figure 4 shows the velocity waveforms and figure 5 the time-averaged velocity at each position along the change of the dimensionless axial position in the downstream direction for three time-averaged Reynolds numbers. Figure 4 shows the turbulent components in most of the phases except the early stage of the accelerating phase and the velocity waveforms that result when the flow proceeds downstram from the inlet part and to the wall from the center of the duct. Figure 5 shows that time-averaged velocity distribution for turbulent pulsating flow are almost unchanged from $x/D_h=40$ after these values are increased more and more in the entrance region. Time-averaged velocity on the centerline are increased according to increasing time-averaged Reynolds number. We can also observe the phenomenon of overshoot at $x/D_h=30$ in Fig. 6. It is considered that inertia force in dominant in this region compared with viscous force. Figure 7 shows the distribution of time-averaged velocities over the fully-developed central time-averaged velocity ($\overline{u}_{ta}/\overline{u}_{ta,cl,fd}$) for each time-abveraged Reynolds number. The velocity distributions of the time-averaged components on the centerline increase more and more and approach the unity in the fully developed region. And these distribution is in good agreement with the one-seventh power law as for the turbulent steady flow. This implies that the turbulent pulsating flow in this experiment can be regarded as a

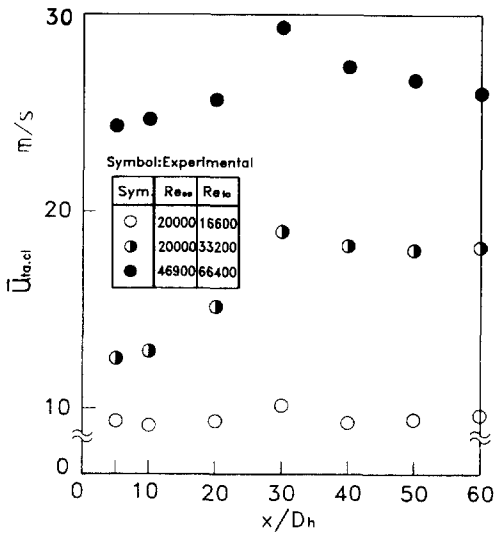

Fig. 6 Time-averaged velocity distribution on the centerline for developing turbulent pulsating flow

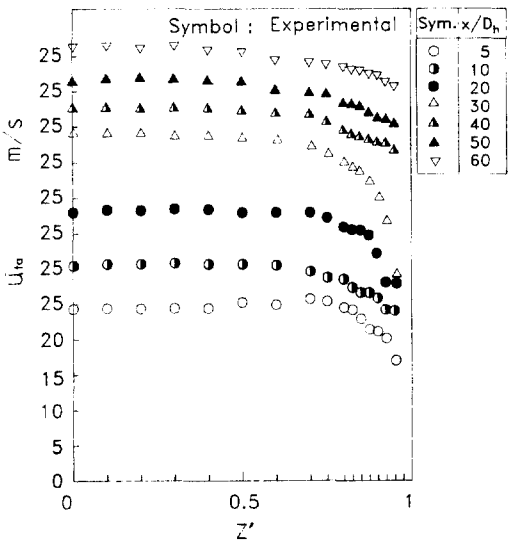

Fig. 5 Cross-sectional velocity profiles of the time-averaged for developing turbulent pulsating flow

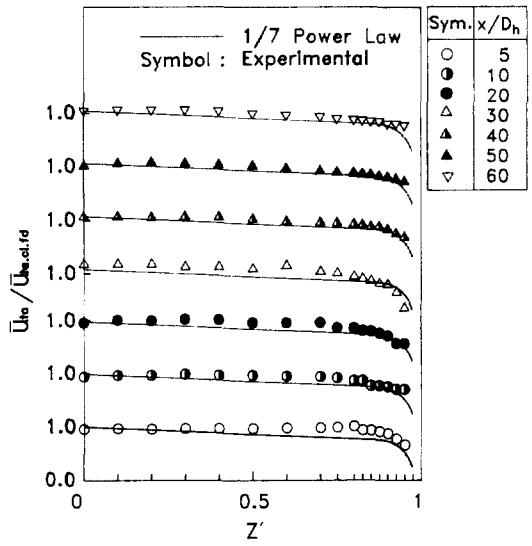

Fig. 7 Distribution of time-averaged velocity divided by fully developed value on the centerline for developing turbulent pulsating flow at $Re_{ta}=66400$ and $Re_{os}=46900$

quasi-steady flow.

Figure 8 shows the distribution of oscillatory components for the position of dimensionless axial direction of the duct. The distribution of oscillating components for turbulent pulsating flow is almost flat in the entrance region, but as the flow progresses downstream the invicid core region disappears. The distribution of oscillatory components over the central fully developed oscillatory velocity for developing turbulent pulsating flow is shown in figure 9. The rate of each oscillating velocity amplitude over that of the center for fully devel-

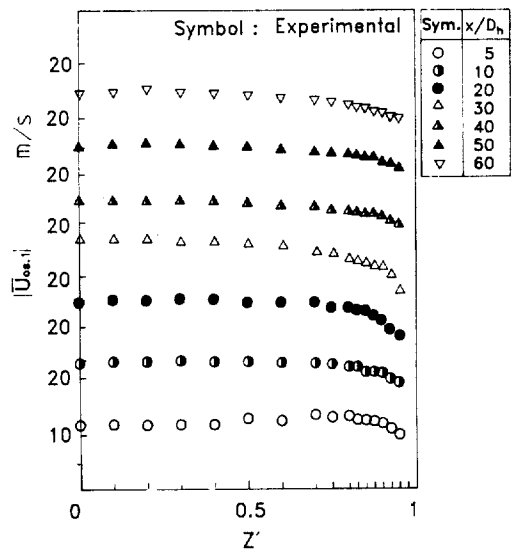

Fig. 8 Distribution of oscillating velocity amplitude for developing turbulent pulsating flow at Re_{ta} =66400 and Re_{os}=46900

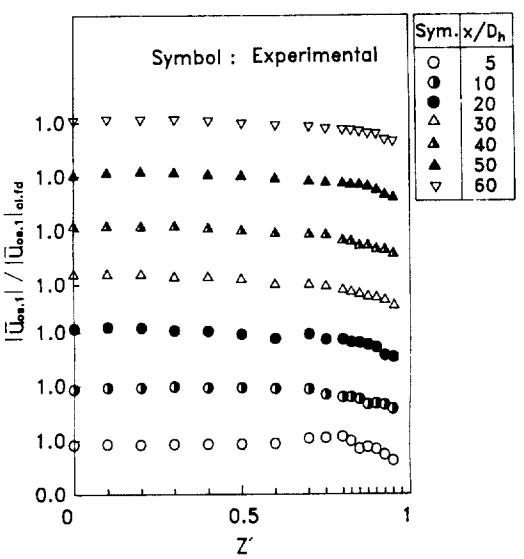

Fig. 9 Distribution of oscillating velocity amplitude divided by fully developed value on the centerline for developing turbulent pulsating flow at Re_{ta}= 66400 and Re_{os}=46900

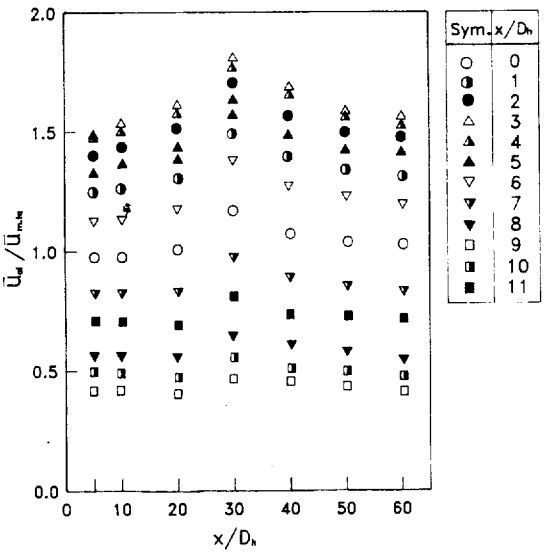

Fig. 10 Velocity distribution on the centerline divided by time-averaged mean velocity for developing turbulent pulsating flow at Re_{ta}= 66400 and Re_{os}=46900

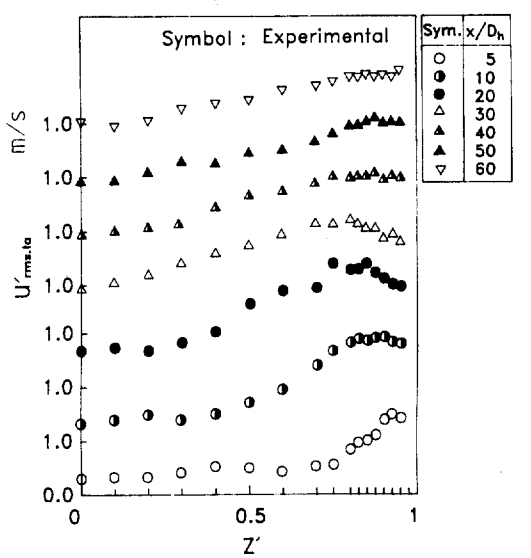

Fig. 11 Distribution of time-averaged root mean square value for developing turbulent pulsating flow at Re_{ta}= 66400 and Re_{os}=46900

oped flow showed the same inclination as in Fig. 8. Figure 10 shows the distributions of the rate of central velocity and time-averaged mean velocity ($\overline{u}_{c1}/\overline{u}_{m,ta}$) along the dimensionless axial position in the downstream direction. From these results, the overshoot phenomenon appears at $x/D_h=30$. In the accelerating phase [$\omega t/(\pi/6)=0\sim3, 9\sim11$], the velocity on the centerline of the duct is gradually developing; the symbols [$\omega t/(\pi/6)$] denote the phases for turbulent pulsating flow.

The distribution of the time-averaged turbulence intensity along the change of cross-sectional and dimensionless axial position in the downstream direction is shown in Fig. 11. This is compared with the time-averaged root mean-square value of the center in the fully-developed duct. From these results we can observe that the time-averaged root mean square values in the turbulent pulsating flow increse more and more in the central part of the duct and decrease more and more in the wall region of the duct along the change of the dimensionless axial position in the region of the duct along the change of the dimensionless axial position in the downstream direction. This phenomenon occurs in the wall by the reason of a larger viscous force as compared with the inertia force. Figure 12 shows the turbulence intensity distributions for turbulent pulsating flow ($u'_{rms}/\overline{u}_{m,ta}$). These distributions show an increase in a straight line neary from the center to the wall of the duct in the inlet region. These distributions do not change in the central part but suddenly in the wall region. Turbulence intensity is large in the phase to have bigger velocity and is smaller in the accelerating than in the decelerating region.

The distributions of $|u'_{rms,os,1}|_{c1}/|u'_{rms,os,1}|_{c1,fd}$ along to the change of demensionless axial position in each time-averaged Reynolds number are shown in Fig. 13. The values of $|u'_{rms,os,1}|_{c1}/|u'_{rms,os,1}|_{c1,fd}$ are increased in the inlet region along the dimen-

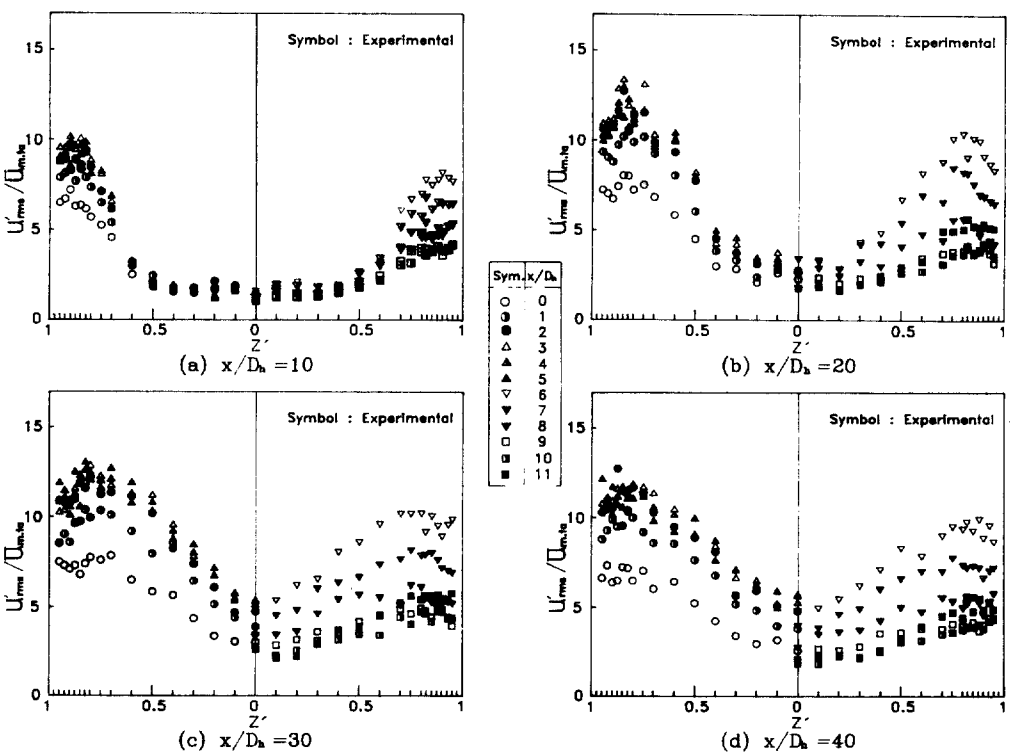

Fig. 12 Turbulence intensity($u'_{rms}/\bar{u}_{m,ta}$) distribution of developing turbulent pulsating flow at Re_{ta}= 66400 and Re_{os}=46900

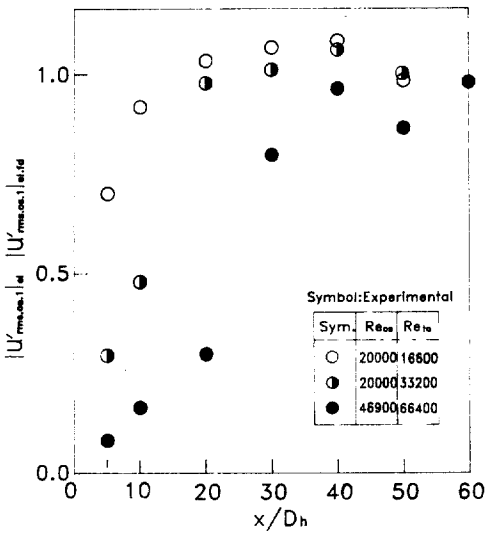

Fig. 13 Distribution of $|u'_{rms,os,1}|_{cl}/|u'_{rms,os,1}|_{cl,fd}$ for developing turbulent pulsating flow

sionless axial postion in the downstream direction and equal to unity in the full developed region. The unity implies that these distributions do not change in the neighborhood of axial position around 40.

4. Conclusion

The results obtained from the experimental study on developing turbulent pulsating duct flow are as follows:

(1) The time-averaged component of the turbulent pulsating flow agrees well with the one-seventh power law in the fully developed region, just as with turbulent steady flow, and the overshoot phenomenon occurs at the location of dimensionless axial direction (x/D_h) equal to 30 in the turbulent steady flow.

(2) The distribution of turbulence intensity in turbulent pulsating flow ($u'_{rms}/\bar{u}_{m,ta}$) showed a linear increase as it went from the center of the duct to the wall, as in the case of the turbulent steady flow. Turbulence intensity was slightly smaller in the acceleration than in the deceleration phase.

(3) The entrance length of the turbulent pulsating flow is very little influeced by the time-averaged Reynolds number of the turbulent pulsating flow. The location where the velocity distribution for axial direction is nearly invariant was about 40 times the hydraulic diameter.

Reference

(1) Gessner, F.B.,, Po, J.K., and Emery, A.F., 1977, "Measurement of Developing Turbulent Flows in a Square Duct," Univ. of Washington, pp. 119~136.

(2) McComas, S.T., 1967, "Hydrodynamic Entrance Lengths for ducts of Arbitary Cross Section," J. of Basic Eng., pp. 847~850.

(3) Iguchi, M. and Ohmi, M., 1983, "Turbulent Acclerating and Decelerating Pipe Flows in Quasi-Steady Motion," Osaka Univ., Vol. 33, No. 1696, pp. 97~106.

(4) Iguchi, M. and Ohmi, M., 1983, "Unsteady Frictional Losses in Decelerating Turbulent Pipe Flows," Osaka Univ., Vol. 33, No. 1728, pp. 349~358.

(5) Ohmi, M. and Iguchi, M., 1980, "Flow Pattern and Frictional Losses in Decelerating Pipe Flow; Part 3 General Representation of Turbulent Frictional Losses," Bul. of the JSME, Vol. 23, No. 186, pp. 2029~2036.

(6) Ohmi, M. and Iguchi, M., 1987, "Flow Pattern and Frictional Losses in Pulsating Pipe Flow; Part 4 General Representation of Turbulent Frictional Losses," Bul. of the JSME, Vol. 24, No. 187, pp. 67~74.

(7) Park, G. M., 1987, "Flow Characteristics of Developing Laminar Unsteady Flow in a Square Duct," Ph. D. Thesis, Korea Univ.

(8) Yoo, Y. T., 1990, "A Study on Flow Characteristics of Developing Transitional Steady, Oscillatory and Pulsating Flows in the Entrace Region of a Square Duct," Ph. D. Thesis, Chosun Univ.

(9) Koh, Y. H., 1992, "A Study on Turbulent Characteristics of Developing Turbulent Steady and Unsteady Flows in the Entrance Region of a Square Duct," Ph. D. Thesis, Chosun Univ.